An empirical formula for scattered neutron components in fast neutron radiography*

DOU Hai-Feng(窦海峰)[1)] TANG Bin(唐彬)

Institute of Nuclear Physics and Chemistry, China Academy of Engineering Physics, Mianyang 621900, China

Abstract: Scattering neutrons are one of the key factors that may affect the images of fast neutron radiography. In this paper, a mathematical model for scattered neutrons is developed on a cylinder sample, and an empirical formula for scattered neutrons is obtained. According to the results given by Monte Carlo methods, the parameters in the empirical formula are obtained with curve fitting, which confirms the logicality of the empirical formula. The curve-fitted parameters of common materials such as ^{6}LiD are given.

Key words: fast neutron radiography, scattered neutrons, empirical formula

PACS: 89.20.Bb, 89.20.Dd **DOI:** 10.1088/1674-1137/35/5/016

1 Introduction

Fast neutron radiography (FNR) offers a powerful nondestructive inspection tool for evaluating the integrity of thickly sealed targets. This is particularly true in detecting voids, cracks or other defects in low-Z materials (e.g. plastics, ceramics, etc.) that are shielded by thick, high-Z parts [1]. Since it can easily penetrate high-Z materials, fast neutrons, by interacting with low-Z materials, may yield clear and detailed images that are difficult to duplicate with either X-ray or thermal neutrons. Therefore, FNR is considered an important tool in the area of nuclear stockpile stewardship [2]. The goal for FNR's future development is to develop and deploy an imaging system capable of detecting cubic-mm-scale structural defects in the low-Z materials shielded by thick, high-Z parts [3].

An effect of contrast distortion in the image could be explained by neutron source distortion due to scattered neutrons that originate from the object and the environment [4, 5]. The estimation of the scattered neutron component is necessary. In this paper, a simplified formula for the scattered neutron component originating from the object is developed.

2 Theoretical analysis

2.1 Modeling

A simplified cylinder model (with two dimensional parameters: axis size and radius size) filled with only one kind of material, for example ^{238}U, is assumed to estimate the component of scattered neutrons originating in the object for the sake of pre-simplification. Incident fast neutron beams are parallel and the incident neutrons attenuate in the cylinder sample. The model and the parameters are shown in Fig. 1.

The mechanism of the interplay between fast neutrons and the materials is complex. The scattering reaction, absorbing reaction, and reacting rate are different for different materials, which are related to the energy of fast neutrons. Fast neutrons are always scattered while they are interacting with most common matter. When fast neutrons penetrate thick matter, the energy attenuation and the deviation of incident neutron direction could be considered as the incident neutron adsorption. So it is an approximate analysis taking the attenuation while fast neutrons penetrate an object as decaying exponential.

The model is based on some other assumptions:

Received 27 July 2010

* Supported by Science and Technology Development Foundation of CAEP (2008B0103002)

1) E-mail: douhf@sina.com

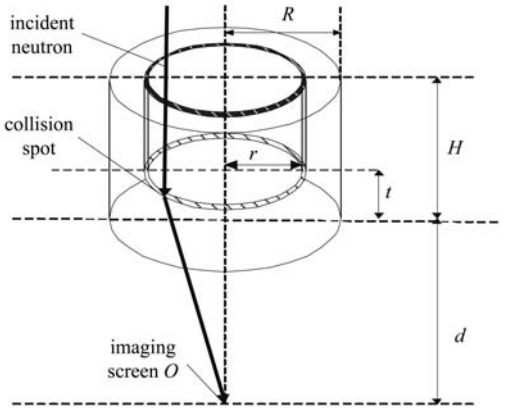

Fig. 1. A simple model for scattered neutrons in FNR. H-Thickness of sample; t-Distance between the collision spot and the bottom of the sample; R-Radius of sample; r-Distance between the collision spot and the axis of the sample; d-Distance between the sample and the imaging screen.

1) Only a single scattering process is considered. The multiple scattering neutrons are treated as being absorbed (The cross section of a fast neutron is always smaller, so the multiple scattering probability is relative low).

2) The object is an isotropic scattering medium according to fast neutrons.

3) The scattered neutrons are attenuated in the sample with the same attenuation factor as the incident neutrons. This means that the cross section of scattered neutrons is equal to that of the incident neutrons.

We now assume that the area where the incident neutrons scatter (see Fig. 1) is sufficiently small, and all scattering neutrons in the infinitesimal volume travel along the same path towards the spot O. According to the above model being axisymmetric, the area is

$$\mathrm{d}S = 2\pi r \cdot \mathrm{d}r. \tag{1}$$

The first collision probability in the area is given by

$$P(t) = \mathrm{e}^{-\Sigma_t (H-t)} \cdot \Sigma_\mathrm{s}. \tag{2}$$

The probability that the scattering neutrons travel in the direction to O spot is

$$P_1(t) = \frac{1}{4\pi\left[r^2+(t+d)^2\right]} \times \frac{t+d}{\sqrt{r^2+(t+d)^2}}. \tag{3}$$

The probability that the scattering neutrons travel to the crack pixel without another collision is

$$P_2(t) = \mathrm{e}^{-\Sigma_t \frac{t}{t+d}\sqrt{r^2+(t+d)^2}}. \tag{4}$$

The total scattered neutron intensity on spot O shown in the Fig. 1 is obtained by Eq. (5),

$$\begin{aligned} I_s &= \int_0^H \int_0^R I_0 \mathrm{d}S \times P(t)\mathrm{d}t \times P_1(t) \times P_2(t) \\ &= \int_0^H \int_0^R I_0 \Sigma_\mathrm{s} r \frac{t+d}{2\left(r^2+(t+d)^2\right)^{3/2}} \\ &\quad \times \mathrm{e}^{-\Sigma_t (H-t)} \mathrm{e}^{-\Sigma_t \frac{t}{t+d}\sqrt{r^2+(t+d)^2}} \mathrm{d}t\mathrm{d}r, \end{aligned} \tag{5}$$

where I_0, I, Σ_t and Σ_s mean incident neutron flux, scattered neutron flux on the origin O, total macroscopic cross section of the sample and macroscopic scattering cross section of the sample, respectively.

2.2 Simplification

At first, the scattered neutron components from different samples with different thickness or different radius are separately simulated with Monte Carlo methods [6, 8]. The energy of incident neutrons is 14 MeV. The ratio of the number of scattered neutrons originating in the sample with a radius of 6 cm to the number of penetrating neutrons (for short, scattering rate) as a function of the thickness is shown in Fig. 2(a). The scattering rate as a function of the radius of the sample with a thickness of 6 cm is shown in Fig. 2(b).

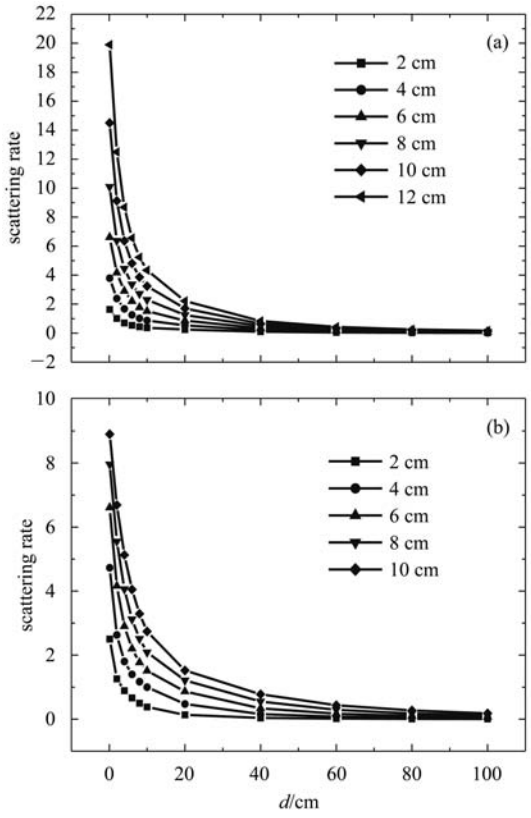

Fig. 2. The scattering rate of samples with different thickness (a) and different radius (b).

Figure 2 shows two points, as follows:

1) The scattering rate decreases as the distance between the sample and the imaging screen increases. When the distance between the sample and the imaging screen gets to about 100 cm, the scattering rate falls slowly. So the distance between the sample and the imaging screen is always set at 100 cm to reduce the number of scattered neutrons. The parameter d is assumed to be much larger than parameter R and H during simplification.

2) The scattering rate increases along with the increment of radius dimension or thickness. And it is more obvious when the thickness increases. So parameter R is approximately simplified.

The parameter R is considered much smaller than d because d is always set more than 100 cm in the FNR experiments. So Equation 1 is developed based on the Gauss-Legendre theory:

$$I = \frac{I_0\Sigma_s}{2}\int_0^H \left[\frac{\frac{5}{9}\frac{R}{2}\left(1+\frac{\sqrt{15}}{5}\right)}{(t+d)^2}e^{-\Sigma_t H}+\frac{\frac{5}{9}\frac{R}{2}\left(1-\frac{\sqrt{15}}{5}\right)}{(t+d)^2}e^{-\Sigma_t H}+\frac{8}{9}\frac{R}{2}\frac{1}{(t+d)^2}e^{-\Sigma_t H}\right]dt$$

$$= \frac{I_0\Sigma_s}{2}\int_0^H \frac{R}{(t+d)^2}e^{-\Sigma_t H}dt = \frac{I_0\Sigma_s R}{2}e^{-\Sigma_t H}\frac{H}{d(d+H)}. \quad (6)$$

In view of the unitary character of Monte Carlo methods, the neutron count per starting particle (I_u) is obtained,

$$I_u = \frac{I}{I_0\pi R^2} = \frac{I_0\Sigma_s R}{2}e^{-\Sigma_t H}\frac{H}{d(d+H)}\times\frac{1}{I_0\pi R^2}$$

$$= \frac{\Sigma_s}{2\pi R\Sigma_t}\Sigma_t e^{-\Sigma_t H}\frac{H}{d(d+H)}. \quad (7)$$

Ignoring the multiple scattering neutrons and the total cross section adopted in development including elastic cross-section, inelastic cross-section, etc, two undetermined coefficients C_1, C_2 are added to the empirical formula. Now the empirical formula is shown as

$$I_u = C_1\frac{\Sigma_t}{R}e^{-C_2\Sigma_t H}\frac{H}{d(d+H)}. \quad (8)$$

3 Data analysis

It is difficult to measure the scattered neutron separately, so the simulation of FNR by Monte Carlo methods is developed first. The curve fitting is then obtained according to the calculation results.

Firstly, the curve fitting of the scattering rate as a function of sample thickness is obtained and shown in Fig. 3 in accordance with the simplification results.

The results of curve fitting are obtained as shown in Fig. 3. C_1=12.29464, C_2=0.62901. The scattered neutron rate of the origin O is obtained from Eq. (8),

$$I = 12.29464\frac{\Sigma_t}{R}e^{-0.62901\Sigma_t H}\frac{H}{d(d+H)}. \quad (9)$$

Comparison of the curve given by formula (9) with

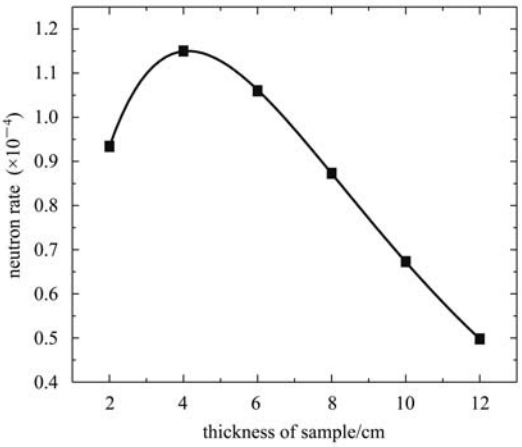

Fig. 3. A curve fitting of scattering rate as a function of sample thickness.

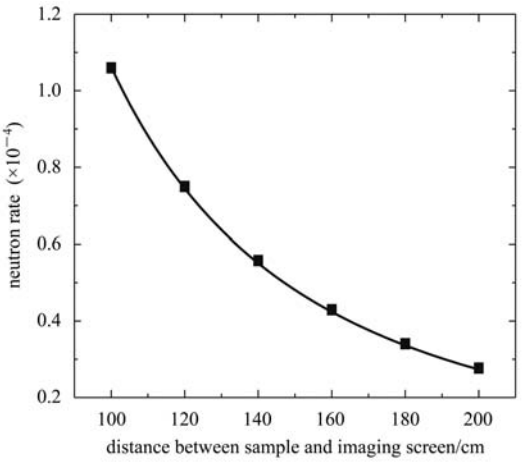

Fig. 4. Comparison between the data curve obtained from formula (9) and the data points calculated by Monte Carlo methods as a function of different distance between the sample and the imaging screen.

the scattered neutron rate as a function of d is shown in Fig. 4 (The data of the scattered neutron rate as a function of d is obtained by Monte Carlo methods).

Figure 4 shows that the scattered neutron rate as a function of d calculated with Monte Carlo methods is consistent with the curve given by formula (9). That is to say, the empirical formula given above is logical. The fitting coefficients based on the simulation results as a function of H are consistent with those based on the simulation results as a function of parameter d.

The fitted curves of some common materials are analyzed. The results are shown in Figs. 5–8. It is proved that the empirical formula is widely applicable.

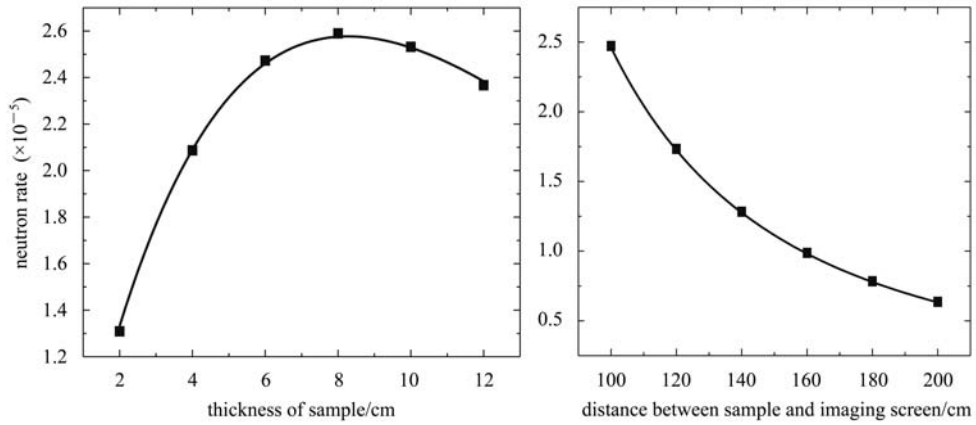

Fig. 5. The fit curve and data calculated with Monte Carlo methods of the ^{6}LiD sample.

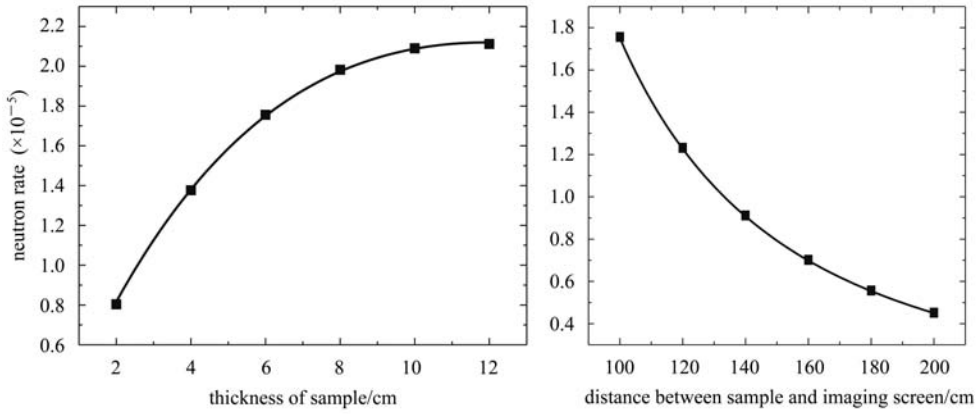

Fig. 6. The fit curve and data calculated with Monte Carlo methods of the $(C_2H_2)_n$ sample.

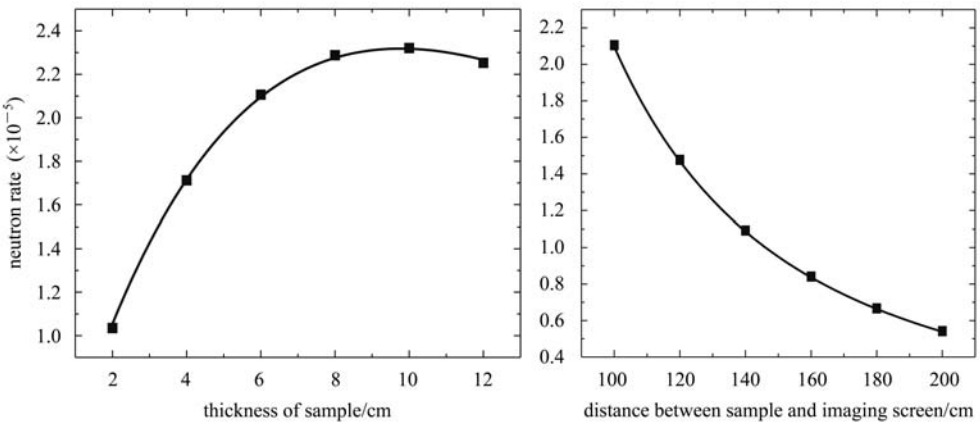

Fig. 7. The fit curve and data calculated with Monte Carlo methods of the ^{6}LiH sample.

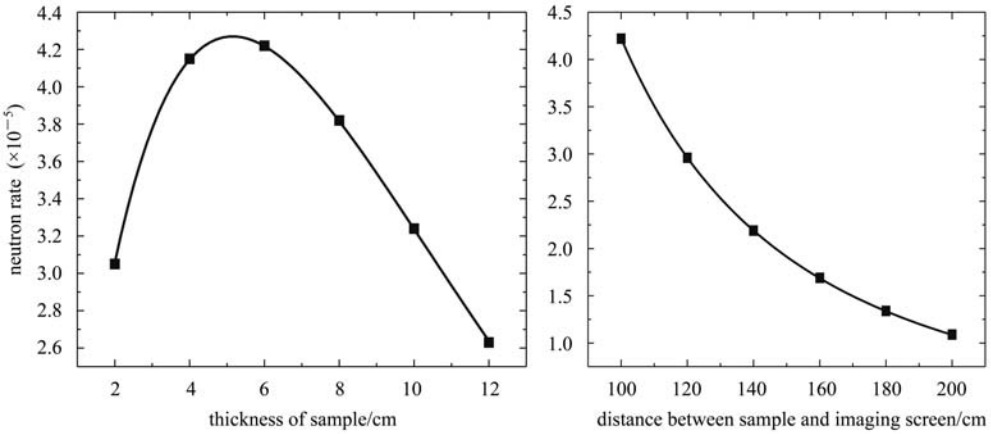

Fig. 8. The fit curve and data calculated with Monte Carlo methods of the Fe sample.

The results of the coefficient fit are shown in Table 1.

Table 1. Coefficient fit of some common materials.

material	$(C_2H_2)_n$	^{6}LiH	^{6}LiD	^{56}Fe	^{238}U
parameter $C1$	1.03947	1.27227	1.91829	5.01585	12.29464
parameter $C2$	0.26675	0.30527	0.42022	0.68334	0.62901
$\Sigma_t/\mathrm{cm}^{-1}$	0.278909	0.305576	0.265583	0.270132	0.282743

4 Conclusion

The simplified empirical formula of scattered neutron rate in FNR is developed, with which the curve fitting of data calculated by Monte Carlo methods is processed. The fitting coefficients based on the simulation results as a function of H are always consistent with those based on the simulation results as a function of parameter d. This validates the simplified formula. At the same time, the parameters of some common materials are given. The universality of the formula is validated and the parameters can be applied to meet the requirements of approximately estimating the distance between the sample and the imaging screen.

Because of omitting the multiple scattering neutrons and the neutron multiplication reactions in the mathematic model, both the coefficient C_1 being quite far from $\dfrac{\Sigma_\mathrm{s}}{2\pi\Sigma_t}$ and the coefficient C_2 being certainly smaller than 1 can be expected. Consequently, the coefficients of a sample cannot be applied to another material.

It deserves attention that the formula should be applied in the case of $R \ll d$. And regretfully, the formula cannot be applied to estimate the intensity of scattered neutrons as a function of R.

References

1 Kinney H, Kim et al. Nuclear Instruments and Methods in Physics Research A, 1999, **422**: 929–932
2 Takenaka N et al. Nuclear Instruments and Methods in Physics Research A, 1999, **424**: 73–76
3 Drell S et al. Science Based Stockpile Stewardship. National Technical Information Service. 1994, 111
4 James Hall (PI) et al. High-Energy Neutron Imaging Development at LLNL. FY06 Annual Report submitted for ESC project LL-24, United States, USDOE, 2006. 15
5 Koji Yoshii, Hisao Kobayashi. Nuclear Instruments and Methods in Physics Research A, 1996, **377**: 76–79
6 Frank Dietrich et al. AIP Conf. Proc., 1997, **392**: 837–840
7 Rahmanian H et al. Nuclear Instruments and Methods in Physics Research Section A, 2002, **477**: 378–382
8 Matsubayashi Masahito, Hibiki Takashi et al. Nuclear Instruments and Methods in Physics Research A, 2004, **533**: 481–490